



A theoretical study on the hydraulic conductivity of anisotropic granular materials by implementing the microstructure tensor

Mehdi Veiskarami¹ · Leila Roshanali¹ · Ghassem Habibagahi¹

Received: 21 April 2023 / Accepted: 21 June 2023 / Published online: 3 August 2023
© The Author(s), under exclusive licence to Springer-Verlag GmbH Germany, part of Springer Nature 2023

Abstract

A theoretical study on the hydraulic conductivity of fully saturated anisotropic granular materials for a 2D fluid flow has been made by making use of the microstructure tensor as the anisotropy descriptor. The assemblage of particles was assumed to be the representative elementary volume of materials with void spaces as a multiply-connected continuum through which a Stokesian flow can pass. The Navier–Stokes equations have been then solved to find the mean velocity vector under different pressure boundary conditions. A tensorial form of the hydraulic conductivity with constants being functions of the invariants of the microstructure tensor, as the geometric measure of the anisotropy, has been presented based on a number of realizations for different GSD curves. Verifications with available experimental data exhibit a reasonable accuracy of the suggested equation.

Keywords Anisotropy · Fluid flow · Granular materials · Hydraulic conductivity · Microstructure tensor · Navier–Stokes equations · Porosity

1 Introduction

The hydraulic conductivity of porous media, as a very challenging problem, finds its roots in historical work of Darcy [10] with applications in many disciplines [6, 12, 29]. Afterwards, a variety of methods were developed to study the hydraulic conductivity in granular porous media, mainly for isotropic materials; among which are the empirical works of Hazen [19] and Slichter [52]. Later, Kozeny [27] and Carman [3] followed by Saffman [51] further developed the issue and suggested more elaborative equations for the hydraulic conductivity involving some factors such as the dynamic viscosity, void ratio, specific surface area, unit weight of the permeant or the tortuosity. Unfortunately, measurements on some of factors like the specific surface area, the Kozeny–Carman empirical coefficients or the

tortuosity are often very difficult or inaccurate. Afterwards, simpler equations were suggested with less complications [5, 15, 26, 31]. The study on the hydraulic conductivity is still an open topic in recent years [13, 21, 47, 50, 54]. A bibliography on this topic is presented in Supplement A. Among many, the volumetric porosity (or the void ratio) and the effective grain size have been employed in almost all equations whereas the fluid viscosity, the density and the tortuosity have been found to be less widely used.

Despite the importance, very little attempt has been made to develop an equation for the hydraulic conductivity of anisotropic soils. Of course, some few experimental studies have been conducted to measure the hydraulic conductivity along different directions (e.g. [46]). It is worth noting that the hydraulic conductivity is a tensorial measure [33, 56] and hence, it must be expressed as a tensor quantity. Considering the anisotropic nature of many geomaterials, estimation of this tensor is highly important while challenging.

As the relative position of grains controls the characteristics of a granular medium, different assemblages of particles, corresponding to a fixed Grain Size Distribution (GSD) curve, lead to different hydraulic conductivities. For a class of clean, granular soils with fairly round particles and very little amount of fine grains, the geometry of the pore space, i.e. its spatial and directional distributions, adequately

✉ Mehdi Veiskarami
mveiskarami@gmail.com; mveiskarami@shirazu.ac.ir

Leila Roshanali
leila.roshanali@gmail.com

Ghassem Habibagahi
habibg@shirazu.ac.ir

¹ School of Engineering, Shiraz University, Shiraz, Iran

defines its hydraulic conductivity. A geometric measure can characterize the role of scattering of pore spaces. Here, a practical measure of anisotropy is employed for the medium, called the microstructure tensor, based on the directional porosity of materials, with wide applications in the mechanics of porous materials [22, 30, 34, 35, 43–45]. It was first introduced by Pietruszczak and Krucinski [41, 42] following Kanatani [24], with a technique to measure the density of pores.

In this research, a rational study on the hydraulic conductivity of inherently anisotropic granular materials has been made with assumption that the flow does not further affect the structure of the medium. To do so, a synthetic database of the hydraulic conductivity of a series of anisotropic soils have been developed by solving the Navier–Stokes equations in different assemblages of particles. The flow has been assumed to be two-dimensional which is very common in geotechnical engineering (e.g. in earth dams, groundwater flow, etc., where the flow is more or less the same in parallel planes.) Therefore, the anisotropy can be envisioned as the transversal isotropy. To study the hydraulic conductivity of an anisotropic medium, a number of different particle arrangements have been developed for certain GSD curves. Every arrangement is used to constitute a Representative Elementary Volume (REV) of the soil matrix with a number of randomly distributed grains for a fixed GSD curve and porosity but different measures of anisotropy. The volume averaging technique is applied to study the mean velocity in the fully saturated REV [16, 18, 56] in order to make a database for the velocity vector. Finally, these velocity vectors were related to the hydraulic gradients through a rational tensorial relationship for the hydraulic conductivity. The procedure was compared with analytical solutions and also with some experimental test results available in the literature. The final form of the suggested equation for the hydraulic conductivity was found to be simple and physically consistent with expectations.

In summary, available equations for the hydraulic conductivity are often based on complex quantities like the shape factor, tortuosity, etc. and their estimates for a specific soil show a very wide range. In addition, while most soils are anisotropic by nature, very limited experimental data is available for such soils with no equation, known to the authors, for their hydraulic conductivity. More to the point, the common approach for the hydraulic conductivity of anisotropic materials is inadmissible when it is examined against principles of continuum mechanics and tensor analysis. The novelty of this paper can be in several aspects: (1) addressing some shortcomings in the common approach for the hydraulic conductivity of anisotropic materials and development of a proof on the inadmissibility of the common equation for the hydraulic conductivity of anisotropic materials, (2) development of a synthetic and

verified database of the hydraulic conductivity of anisotropic materials for a series of GSD curves, (3) development and suggestion of a simple rational equation for the hydraulic conductivity of anisotropic materials in tensorial form, based on only a geometric measure of anisotropy. The hydraulic conductivity, presented in terms of a second order tensor, is reduced to its formal scalar measure upon assuming isotropy.

2 Theory of two-dimensional fluid flow and governing equations

The potential flow and the Stokesian flow are two common types of flow in soil mechanics. The potential flow governs an irrotational (or curl free) incompressible flow and the Stokes' flow governs the fluid flow with relatively low Reynolds Number, $R_e \ll 1$ [17].

The potential flow leads to the well-known Laplace equation:

$$\text{div } \mathbf{v} = \nabla \cdot \mathbf{v} = \nabla \cdot (\nabla \varphi) = \nabla^2 \varphi = 0, \quad \mathbf{v} = \nabla \varphi = -k\mathbf{i} \quad (1)$$

If the fluid is incompressible (like the water flow in soil), the equations of the steady-state Stokesian flow will be obtained as follows:

$$-\frac{1}{\rho} \nabla p + \mathbf{b} + \nu \nabla^2 \mathbf{v} = 0 \quad (2)$$

In these equations, $\nu = \mu/\rho$ is the kinematic viscosity, μ is the dynamic viscosity constant, ρ is the mass density of the fluid, \mathbf{v} is the velocity, φ is some fluid potential function, \mathbf{i} is the hydraulic gradient, k is the coefficient of hydraulic conductivity (here, in the particular case of an isotropic body, is a scalar), $R_e = \rho v L/\mu$ is the Reynolds Number (with L being some characteristic length), \mathbf{b} is the body force and ∇ is the gradient (or del) operator.

The finite element technique is often employed to numerically solve these equations [48, 57] with a summary of equations in the supplements of this paper.

3 Outline of the problem and basic assumptions

Characteristics of a porous medium are mainly governed by the relative position of the grains. For instance, a variety of assemblages of particles can be imagined using a particular GSD. Therefore, many characteristics of the medium such as the hydraulic conductivity, can be attributed to the GSD as well as the particles arrangement. In this research, we formally assume that the soil matrix is composed of clean granular materials with very small fine contents and with fairly round particles. For such materials, the effect of fine

fraction and particles shape on the formation of the flow are insignificant. A rational tensorial relationship between the microstructure tensor and the hydraulic conductivity is sought. In absence of sufficient experimental data, numerical simulations were performed on soils with different GSD curves to replace the tedious laboratory sample preparations and several experiments for various flow directions.

Different soil matrices for a particular GSD curve were generated for this purpose, ranging from a nearly isotropic to highly anisotropic which are called *realizations*. These matrices, possess the same number of soil grains and volumetric (or bulk) porosity but different geometric measures of anisotropy. This geometric measure is the microstructure tensor, based on the directional porosity.

To measure the local phenomenon of the hydraulic conductivity by the global phenomenon of the fluid flow, an REV was used to define what is known as a so called material point when working in two scales. Noting that the measurement and scale are closely related [9], for a worthwhile achievement, there is a tradeoff between the size of the REV and the required computational effort with adequate accuracy. By an analogy to the concept of the Knudsen Number, which should be reasonably below 0.1 for a continuum theory or, more precisely, for a slip flow and validity of the Navier–Stokes equations [14], the relative size of the mean grain size, D_{50} , to the size of the REV was limited to 0.05.

Realizations of soil matrices were made in a two-dimensional domain (2D REV), partly for the sake of simplicity and partly due to the importance of two dimensional fluid flow in geotechnical engineering. To justify the two-dimensional studies, the concept of the 2D (area or areal) porosity was employed, i.e. the 3D volumetric porosity was transformed into two dimensions. In general, the two-dimensional (area) porosity is higher than the three-dimensional (volumetric) porosity for a certain soil matrix of some fixed bulk porosity.

For a clear insight, in Fig. 1a, b a three-dimensional assemblage of particles is presented for which, a two-dimensional section is shown with obviously higher void spaces in the plane. Figure 1c illustrates a schematic view of the problem domain with typical prescribed boundary conditions. Figure 1d presents the cross-sections of two closely-spaced parallel planes passing through a relatively dense pack of grains in which, a 2D flow can form. The boundary conditions consist of prescribed pressure (or potential) in order to maintain a steady flow under a unit hydraulic gradient. The finite element mesh is generated to cover the entire void spaces and to find a numerical solution for the velocity field. The velocity vector of the REV, is taken as the mean velocity along the left and right (for the Cartesian component v_x) as well as the top and bottom (for the Cartesian component, v_y) boundaries.

Particles assemblages were generated primarily based on a random process. To do so, one may note that a synthesized assemblage of particles comprises grains of limited sizes as the number of grains and their diameters in a real sample are practically infinitely many. A nearly uniformly graded sand with round particles, can be reasonably represented by a number of 4 to 6 different grain diameters, sampled in equivalent distances along the diameter axis on a GSD curve, with the proportion of the mass in the sample. Thus, the number of each grain size to reproduce an REV of a fixed porosity with limited grain sizes, can be precisely determined by the mass percentage and the porosity of the sample. For example, if the area porosity is 0.64 (equivalent to bulk porosity of 0.5), a sample of three grains of 1 mm, 2 mm and 4 mm would be made up of 6, 3 and 2 grains (or any multiple of them), respectively.

In this research, a series of practical constraints as well as numerical ones were considered to develop the REV and the finite element mesh, i.e. (1) grains are nearly rounded, which means they are either circular or elliptical with the ratio of longer to shorter diameter not greater than 1.5, (2) particles shall not be in contact in the plane of analysis, to enable a free flow formed throughout the REV, (3) distributions are nearly uniform, i.e. small grains are located between large grains, (4) required directional porosity ranges from isotropic to anisotropic materials by inspection of the rose diagram of the directional porosity (nearly circular for isotropic materials while elliptical for anisotropic ones), and (5) the space between two particles must be covered by not less than 2 finite elements (practically, at least by 4 to 6 elements).

While the fourth constraint itself is necessary but the relative orientation of the obtained ellipse (rose diagram) is immaterial as it will be expressed in a tensorial form. The last constraint is a problem in mesh generation and does not directly involve the relative location of particles; however, slight change in the location of particles or jiggling of the mesh often provide a very good space for an efficient mesh generation. This is required to avoid locking of flow in triangular elements. This happens when all nodal points of an elements are located on solid grains and hence, possess no velocity meaning that the flow cannot pass through that element (or that region). A variety of different realizations (or different REV for a fixed material) were generated by randomly changing the location and/or slightly changing the orientation of particles, also by rotating a previously generated REV by ± 90 or 180 degrees. This is important to remind that each realization may also define the character of the material in one of parallel planes for a 2D analysis.

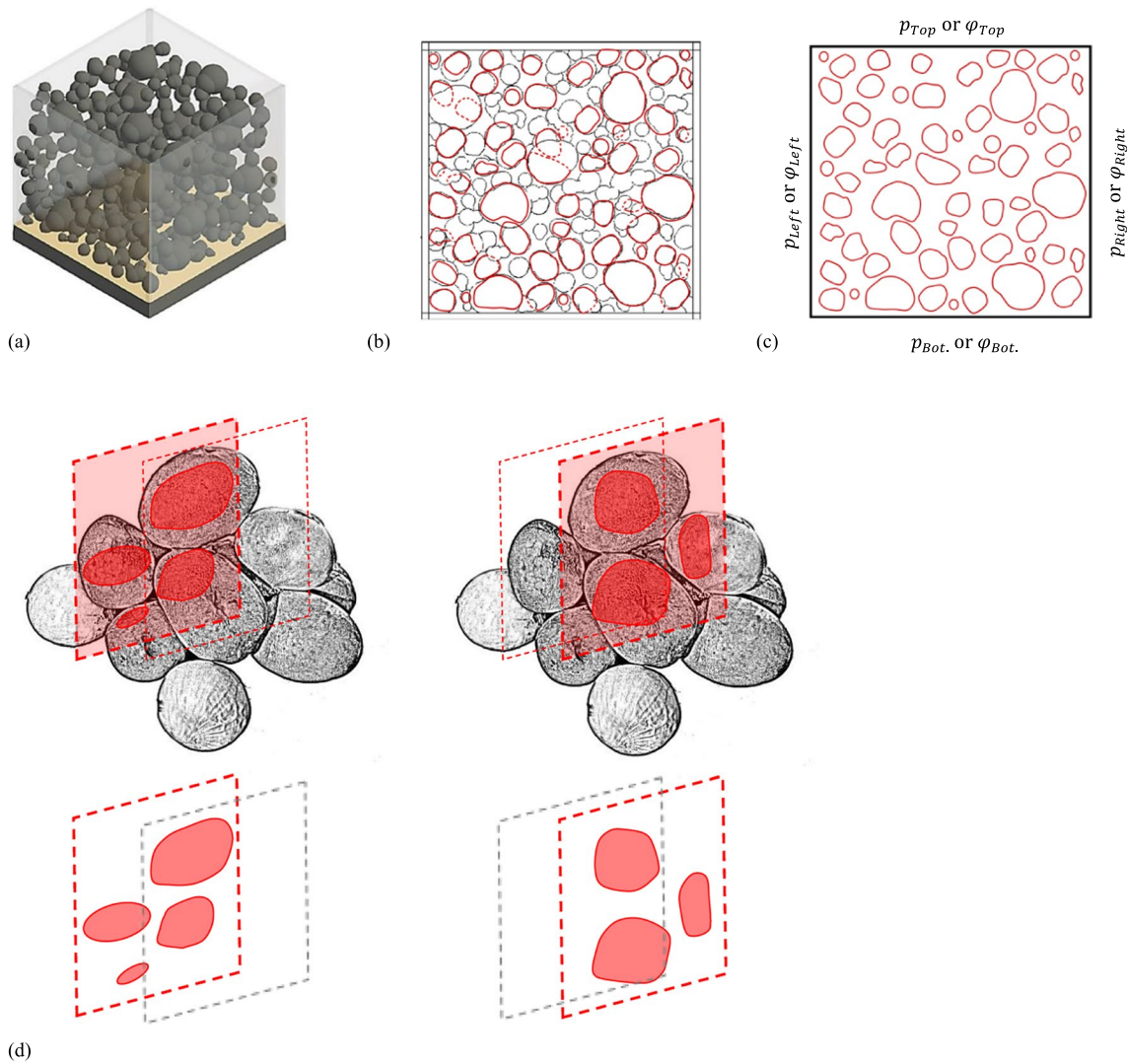


Fig. 1 **a** A 3D assemblage of particles, **b** A 2D assemblage of particles, **c** A 2D cross section within which, the fluid flow analysis is made and **d** a pack of relatively dense particles with two hypothetical

closely-spaced parallel planes showing a schematic view of the 2D cross-sections of these planes

4 A note on the tensorial form of the hydraulic conductivity

A rational proof for the Darcy’s law, stating that it must be expressed as a tensorial form, was made by Neuman [33] and here, we try to extend the concept and relate it to the microstructure tensor. A rational relationship between the geometric measure of anisotropy and the hydraulic conductivity may be visualized as the following tensorial form, with h being the hydraulic head:

$$v = -k \cdot \nabla h \quad \text{where} \quad k = k(\mathfrak{F}) \tag{3}$$

In this equation, \mathfrak{F} , is a geometric measure of anisotropy. Here, this tensorial measure is the fabric tensor (or the microstructure tensor), which will be discussed later. This can be regarded as a generalization of Darcy’s law with k being the hydraulic conductivity tensor with components k_{ij} .

Unfortunately, a misleading equation for the hydraulic conductivity in anisotropic porous media has been often used with the following form, taking the hydraulic conductivity as a scalar quantity along an arbitrary direction, r [8, 11]:

$$\frac{1}{k_r} = \frac{\cos^2 \alpha}{k_x} + \frac{\sin^2 \alpha}{k_y}, \quad v_r = -k_r \partial h / \partial r \tag{4}$$

where, α defines the direction along which, the hydraulic conductivity is calculated. In this equation, no consideration has been made to the partial derivative of h with respect to the other orthogonal coordinate or direction, r . In Appendix 1, it is shown that it violates principles of continuum mechanics for vector quantities, as the velocity vector is no longer transformed like a vector. In other words, v_r depends on k_{rr} as well as k_{rs} . One should also note that k_r with just one index, is meaningless for the 2nd order tensor k_{ij} . Thus, in general, this equation is wrong and cannot be used for the hydraulic conductivity in anisotropic media.

5 The microstructure tensor and the geometric measure of anisotropy

As mentioned before, the microstructure tensor and the way of its measurement date back to studies of Pietruszczak and Krucinski [41, 42] and formerly Oda [36–38]. They considered a unit sphere in the vicinity of a particle and passing hypothetical lines along the diameter of the sphere in different directions passing through void spaces and solids along. The total length of line segments passing the voids, l , is a measure of the directional porosity. In other words, when a trace line passes through a series of pores and solid particles, the total length of line segments in the voids will be l which is obviously less than $2R$. Their ratio, i.e. $L = l/2R$ is a measure of the directional porosity. Figure 2 represents a schematic layout of the unit sphere in the proximity of a material point. The directional porosity can be calculated as [40]:

$$L_{av} = \int_0^{2\pi} \int_0^\pi L(\varphi, \theta) f(\varphi, \theta) d\theta d\varphi, L(\varphi, \theta) = l(\varphi, \theta)/2R \quad (5a)$$

In these equations, $f(\varphi, \theta)$ serves as a function which defines the directions of hypothetical lines to measure the porosity in different directions, $L(\varphi, \theta)$ is the total length of

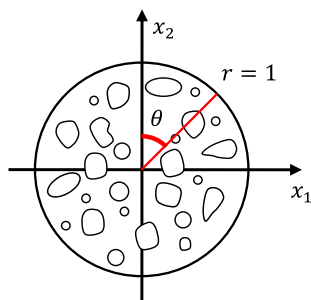


Fig. 2 A 2D section of a soil matrix in a spherical coordinate (r, φ, θ) where the angle φ is out of $x_1 - x_2$ plane and held constant (for a 2D problem)

the pore spaces normalized by the diameter of the sphere, $2R$.

If the lines are uniformly distributed, Eq. (5a) will take the following form:

$$L_{av} = \int_0^{2\pi} \int_0^\pi L(\varphi, \theta) \sin\theta d\theta d\varphi \quad (5b)$$

The fabric descriptor $n(\varphi, \theta)$ or $n^{(m)}$ (which is equivalent to the directional porosity along an arbitrary direction, m), can be calculated as follows [41, 42]:

$$n(\varphi, \theta) = n^{(m)} \cong n_0 (1 + m^T \Omega m), n_0 = L_{av}, n^{(m)} \cong m \cdot \cdot m \quad (6a)$$

$$\cdot \cdot \stackrel{\text{def}}{=} 3n_0 \mathfrak{F}, n^{(m)} \cong 3n_0 m \cdot \mathfrak{F} \cdot m, \mathfrak{F} = \frac{1}{3} (I + \Omega), n_0 = \frac{1}{3} \text{tr} \cdot \cdot \quad (6b)$$

In these equations $n^{(m)}$ is the directional porosity along the unit vector, m , $\cdot \cdot$ is the 2nd order directional porosity tensor, n_0 is the mean porosity (which differs from the volumetric or bulk porosity, n , i.e. the ratio of the volume of voids to the total volume), Ω is a traceless 2nd order tensor (showing the deviation in the directional porosities) which vanishes for isotropic materials and \mathfrak{F} serves as the symmetric microstructure tensor. This equation takes the following form in two dimensions, i.e. where the porosity is in fact the areal (not the volumetric) porosity, $n = n_{2D}$:

$$\cdot \cdot \stackrel{\text{def}}{=} 2n_0 \mathfrak{F}, n^{(m)} \cong 2n_0 m \cdot \mathfrak{F} \cdot m, \mathfrak{F} = \frac{1}{2} (I + \Omega), n_0 = \frac{1}{2} \text{tr} \cdot \cdot \quad (6c)$$

More details can be found in Pietruszczak and Krucinski [41, 42] or Pietruszczak [40]. We use the term volumetric (or bulk) porosity, (n) to distinguish it from the mean porosity (n_0) appeared in the microstructure tensor, as the mean directional porosity. The latter corresponds to the first invariant of the porosity tensor while the former corresponds (or equals) to the third invariant of this tensor, i.e. $n = \det \cdot \cdot$. The plane porosity is also approximated by $n_{2D} = n^{2/3}$. In addition, the directional porosity (geometric measure) is not the only measure of anisotropy; for instance, the distribution of contact points can also be another form of the microstructure tensor. Here, we used the concept of the directional porosity since it is more convenient for the fluid flow problem.

In the present study, directional porosities are measured along a number of trace lines emerged from the center of the REV and the total length of the line segments passing through the void spaces has been calculated for each trace line. Once the tensors $\cdot \cdot$ and Ω , are determined, the fabric tensor (or the microstructure tensor) can be found. In a 2D analysis, some information on the out of plane form of the

pores is embodied in the bulk porosity which indirectly enters the equation for n through $n = n_{3D} = \det n$.

Since Ω is a traceless symmetric tensor, in a 2D analysis, it possesses only two independent components, for instance, Ω_{11} and Ω_{12} . We may define $\eta = n^\theta/n_0 - 1 = \Omega_{11}\cos 2\theta + \Omega_{12}\sin 2\theta$ as a normalized parameter for the directional porosity. Therefore, by making use of a multilinear regression, the best plane passing through these points can be determined to calculate Ω_{11} and Ω_{12} . Thus, the geometric measure of anisotropy in an REV can be found by the concept of the microstructure tensor. In the next step, the numerical solution of the fluid flow in the REV is presented.

6 Numerical analysis and verification with analytical solutions

The flow through void spaces of soil matrices is analyzed by the numerical finite element solution of the Navier–Stokes' equations. In general, triangular CST elements (cf. Reddy 1993; Zienkiewicz and Taylor 1996) were used which seem to satisfactorily cover the complex problem domain throughout the soil matrix. The matrix form of equations is provided in the supplement. The FE procedure was verified for basic requirements such as the partition of unity and modeling of a uniform flow. A fine to very fine mesh (wherever required) has been applied to achieve a very high accuracy in the numerical solution.

Unfortunately, there is no analytical solution for the Navier–Stokes' equations to verify the numerical solution technique. Thus, an attempt was made to verify the numerical procedure for the problem of flow around a circle (or cylinder) for which, at least the potential flow theory can be applied with an analytical solution available. One should note that the flow around a cylinder (even at low velocities) cannot be exactly modelled and all governing equations and solution are only approximates of the actual flow, due to boundary layer effects, formation of vortices, etc. The analytical solution for this flow is only available for an infinite domain. In spite of it, although the Navier–Stokes' and potential flow equations are fundamentally different, their numerical solutions (with similar an almost procedure) are expected to be able to properly model the flow around a circle. In addition, both numerical solutions should reasonably comply with the analytical solution. The analytical solution has been provided by the conformal mapping and complex analysis in an infinite [complex] plane noting that the analytic conformal mapping $w = z + 1/z$, transforms a unit circle to the entire z plane. This helps find an analytical

solution for the potential flow and its velocity field around a circular region, by the following equations [7]:

$$\begin{aligned} w &= z + \frac{1}{z}, & v &= v_x + iv_y = \left(1 - \frac{1}{z^2}\right), \\ \bar{z} &= \text{conj}z, & v &= A \left(1 - \frac{1}{\bar{z}^2}\right) \end{aligned} \quad (7)$$

In these equations, z and w are complex variables defining the coordinates of an arbitrary point in the main problem domain and the transformed domain, respectively, v is the complex velocity vector and A is a coefficient defining the intensity of the flow.

Based on the presented analytical solution, verification has been made for a single grain of a circular shape, illustrated in Fig. 3. Figure 3a shows the outline of the problem and the conformal mapping for the analytical solution. Figure 3b shows the finite element mesh. In order to accurately capture the flow pattern, the domain was taken relatively large with a size ratio of 20 times of the grain diameter. Figure 3c, d show the numerical solutions for potential flow equation and the Navier–Stokes equations, respectively, against the analytical solution in terms of the velocity field. While the potential theory can very accurately model the flow (as expected), the Stokes' flow shows slight deviations due to the fundamental difference between the two governing equations. In spite of it, the global error is still below 2% showing numerical procedure high accuracy. Other examples and verifications are presented in the supplement, still showing high accuracy of the numerical procedure.

Once the solution for a single circular grain was found to be reasonably accurate, further verifications were made to find an optimum relative number of grains and mesh fineness in an REV corresponding to a fixed GSD at a fixed porosity. As stated before, the domain size should be large enough to reasonably reduce the effects of non-homogeneities at grains scale. To do so, an artificial assemblage of particles with three different grain sizes and a fixed area porosity of 0.64 was analyzed. Four to six realizations were made for any of REV's depicted in Fig. 4a. Figure 4b shows the hydraulic conductivity, k_x , calculated for any of these realizations with their average, all normalized by k_x corresponding to the largest REV with the largest relative number of grains. The plot shows that as the domain size grows, the solution becomes more and more stable and the results of realizations tend to a converged value. Here, we mean by the relative number of grains, the ratio of the total number of grains in a pack to those in the smallest unit. The smallest unit (with this relative number equal to 1) contains 2 grains of the largest size, 3 of the medium size and 6 of the smallest size. For a constant porosity and only 3 particle sizes this ratio may involve some slight approximations

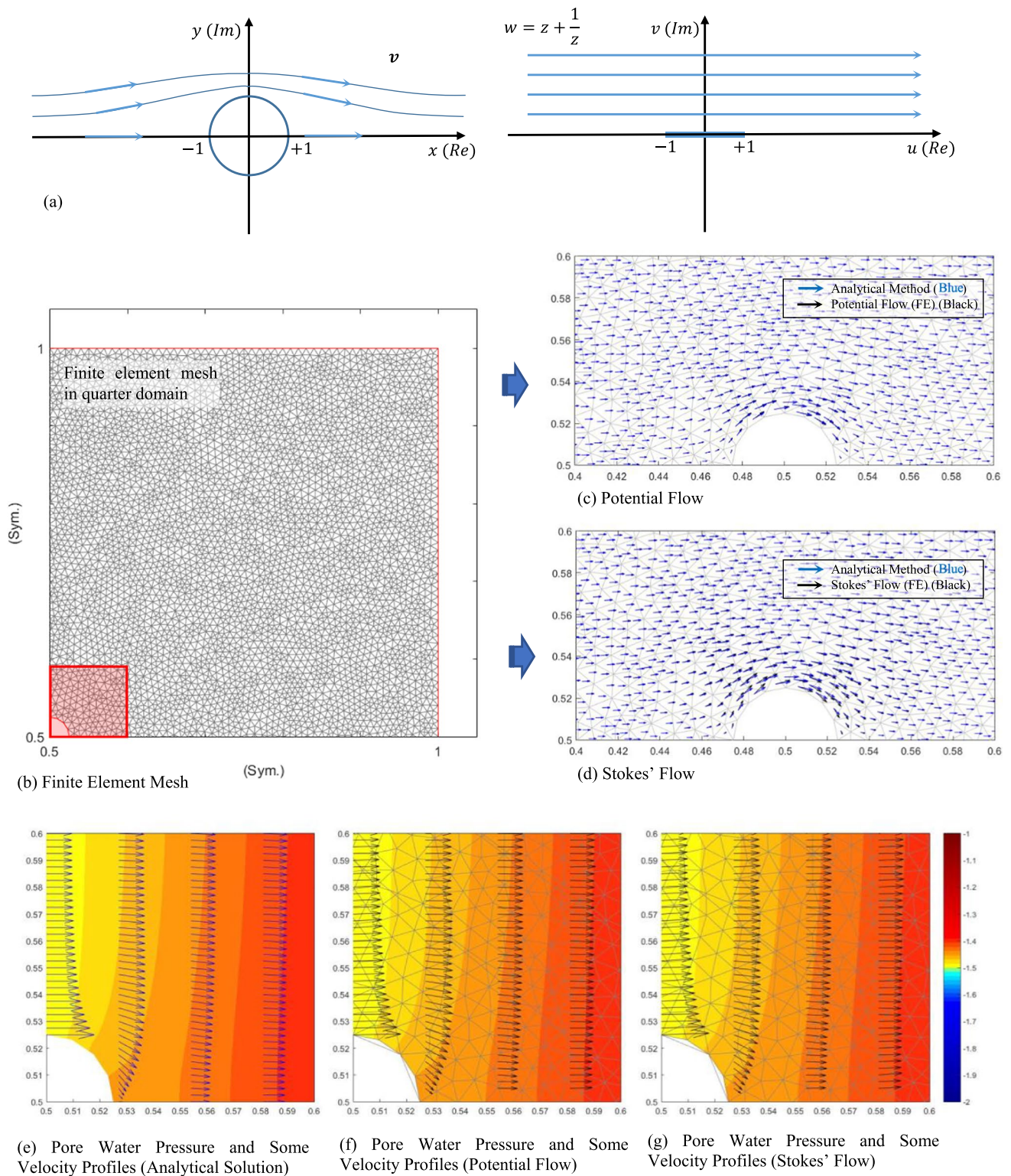
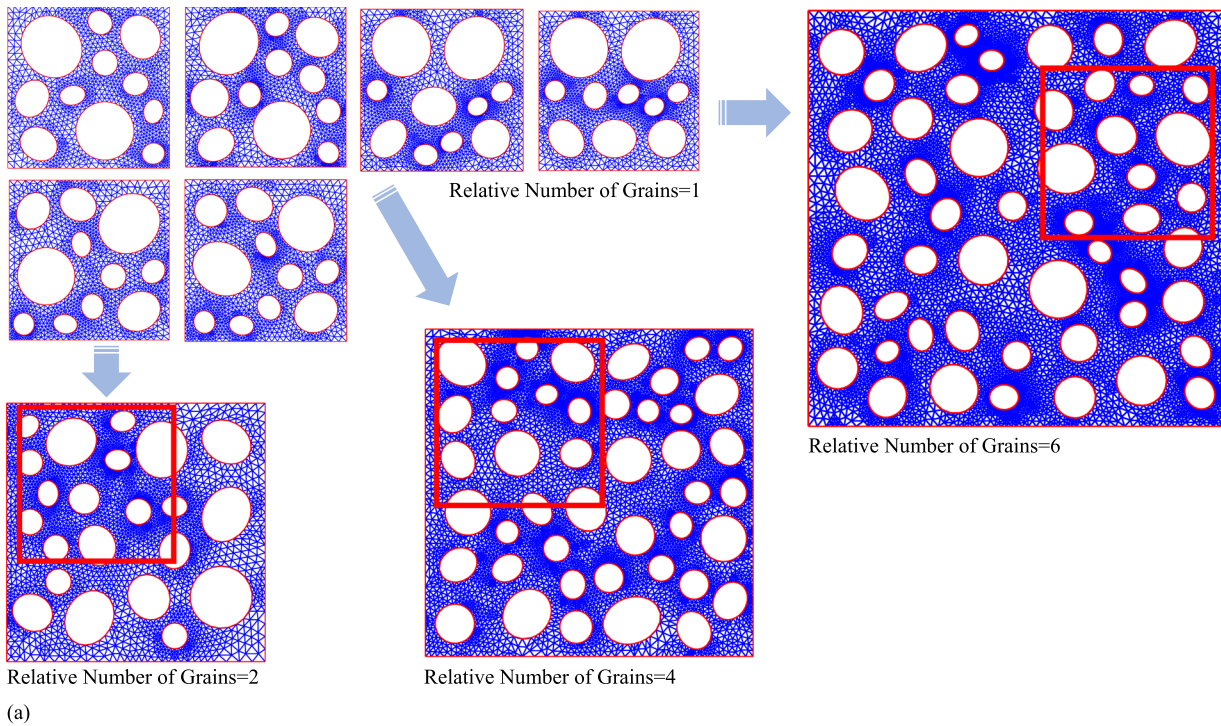
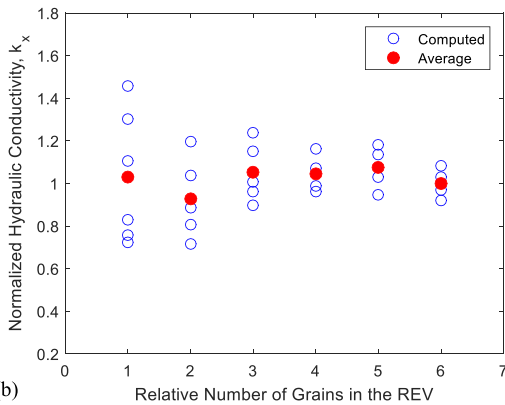


Fig. 3 a Flow around a circular grain, b relatively fine finite element mesh, c numerical and analytical solutions for the potential flow, d numerical and analytical solutions for the Stokesian flow of an incompressible fluid (analytical and numerical velocity fields are in

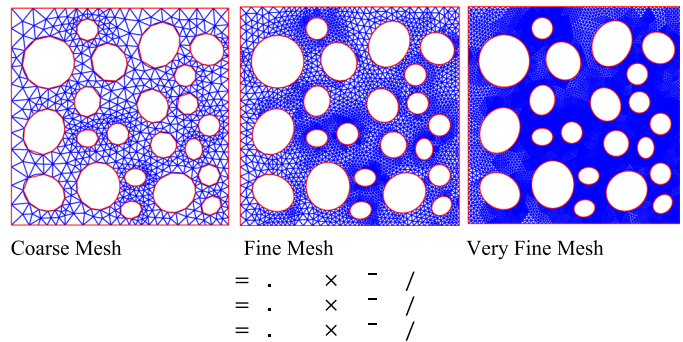
blue and black colors, respectively), e pore water pressure and some velocity profiles (analytical solution), f pore water pressure and some velocity profiles (potential flow) and g pore water pressure and some velocity profiles (Stokes' flow)



(a)



(b)



(c)

Fig. 4 **a** Variety of REV with different number of grains, **b** variations of the hydraulic conductivity with the size of the REV and **c** effect of the finite element mesh coarseness on the hydraulic conductivity

from an integer number. A relative number of grains of 4 and higher, looks reasonable. Figure 4c shows the variation of the hydraulic conductivity for three different mesh sizes. It is evident that a fine mesh has an adequate accuracy, i.e. the solution becomes relatively stable and the difference is well below 10%

with the results for a very fine mesh, which, for the problem under study, sounds to be reasonable. Hereafter, we use a fine mesh with the maximum element size, nearly 1/5 to 1/3 of the smallest grain size.

7 Verification with available experimental data

The numerical solution of the Stokesian flow to calculate the hydraulic conductivity has been verified against some available experimental test results. Attempt has been made to recompile only those experiments on sand (preferably clean sand) with their GSD curves corresponding to medium or coarse sands. For fine grained sands, silts and clays, the assumption of a Stokes' fluid flow will fail to properly model the flow pattern due to the significance of the surface tensions and other factors in fine grained soils. Figure 5, shows the GSD curves of collected samples with their characteristics presented in Table 1. Except one, all samples are clean, almost uniformly graded sands (more precisely, with C_u ranging between 1.5 and 3.5), which are classified as SP according to the Unified Soil Classification

System. The legend of these soils (e.g., S2, S10, S11, SMPM, etc.) are based on their original names found in the corresponding references. Sample SMPM contains a few grains of slightly larger than the maximum size, required for an REV. Despite, as it was the only anisotropic one we found in the literature with required measurements available and as its calibration complies very reasonably with measured data, we included this sample.

A series of assemblages of particles, a minimum of five realizations for each case, with a particular GSD curve and a constant volumetric porosity, have been reproduced. Attempt was made to maintain the isotropy of the assemblage, i.e. it is tried to keep the 2D microstructure tensor close to $I/2$ where I is the isotropic tensor of the second order. This can be visualized by looking at the corresponding rose diagram of each realization which should be close to a circle.

Fig. 5 GSD curves for selected experimental test results (Data from [2, 23, 25, 46])

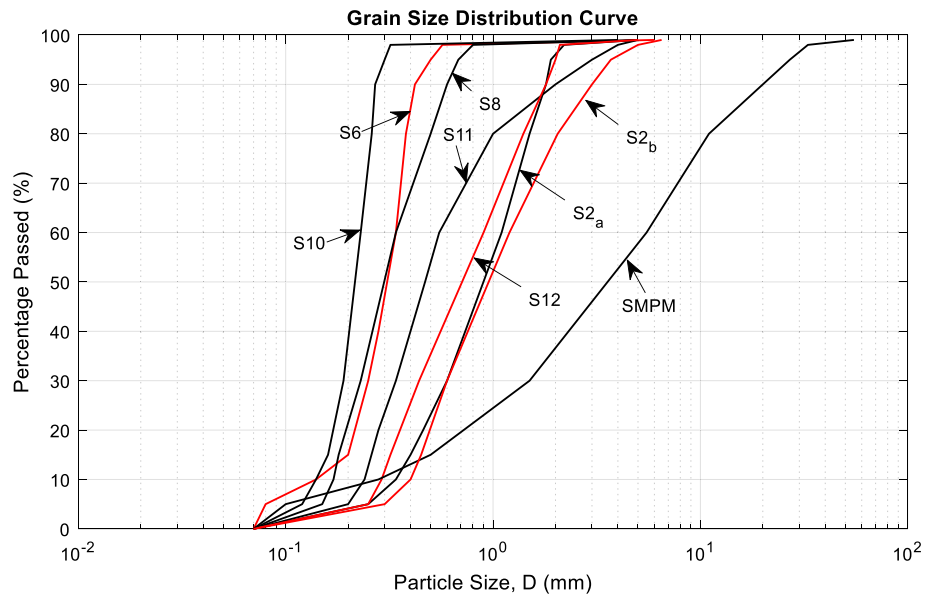


Table 1 Characteristics of the soils used for verifications

Soil type	Volumetric porosity, n	Grain size distribution index Properties (mm)				Uniformity coefficient (C_u)	Unified classification system (USCS)	References
		D_{10}	D_{30}	D_{50}	D_{60}			
S2 _a	0.3809	0.34	0.62	0.98	1.18	3.47	SP	Kedir [25]
S8	0.4222	0.17	0.23	0.29	0.34	2.00	SP	Kedir [25]
S11	0.4157	0.24	0.34	0.47	0.53	2.21	SP	Kedir [25]
S12	0.3884	0.29	0.49	0.76	0.92	3.17	SP	Kedir [25]
SMPM	0.2930	0.15	1.00	2.50	4.20	28.0	SW	Qiu and Wang [46]
S6	0.3500	0.14	0.20	0.29	0.34	2.42	SP	Jaafar and Likos [23]
S10	0.4100	0.17	0.18	0.20	0.21	1.24	SP	Jaafar and Likos [23]*
S2 _b	0.3660	0.30	0.51	0.99	1.04	3.47	SP	Bouteldja et al. [2]

*Data recompiled by Jaafar and Likos [23] based on Nemes et al. [32]

Table 2 Comparison between the predicted and measured hydraulic conductivities of the samples of sand (experiment and report by [25])

Sand type	Porosity, n	Density index, I_D	Grain size distribution index Properties (mm)				Measured hydraulic conductivity, k (m/s)			Predicted hydraulic conductivity, k (m/s)		
			D_{10}	D_{30}	D_{50}	D_{60}	k^{min}	k^{max}	k^{ave}	k^{min}	k^{max}	k^{ave}
S2 _a	0.3809	NA	0.34	0.62	0.98	1.18	NA	NA	3.5×10^{-4}	3.4×10^{-4}	4.2×10^{-4}	3.9×10^{-4}

*NA not available

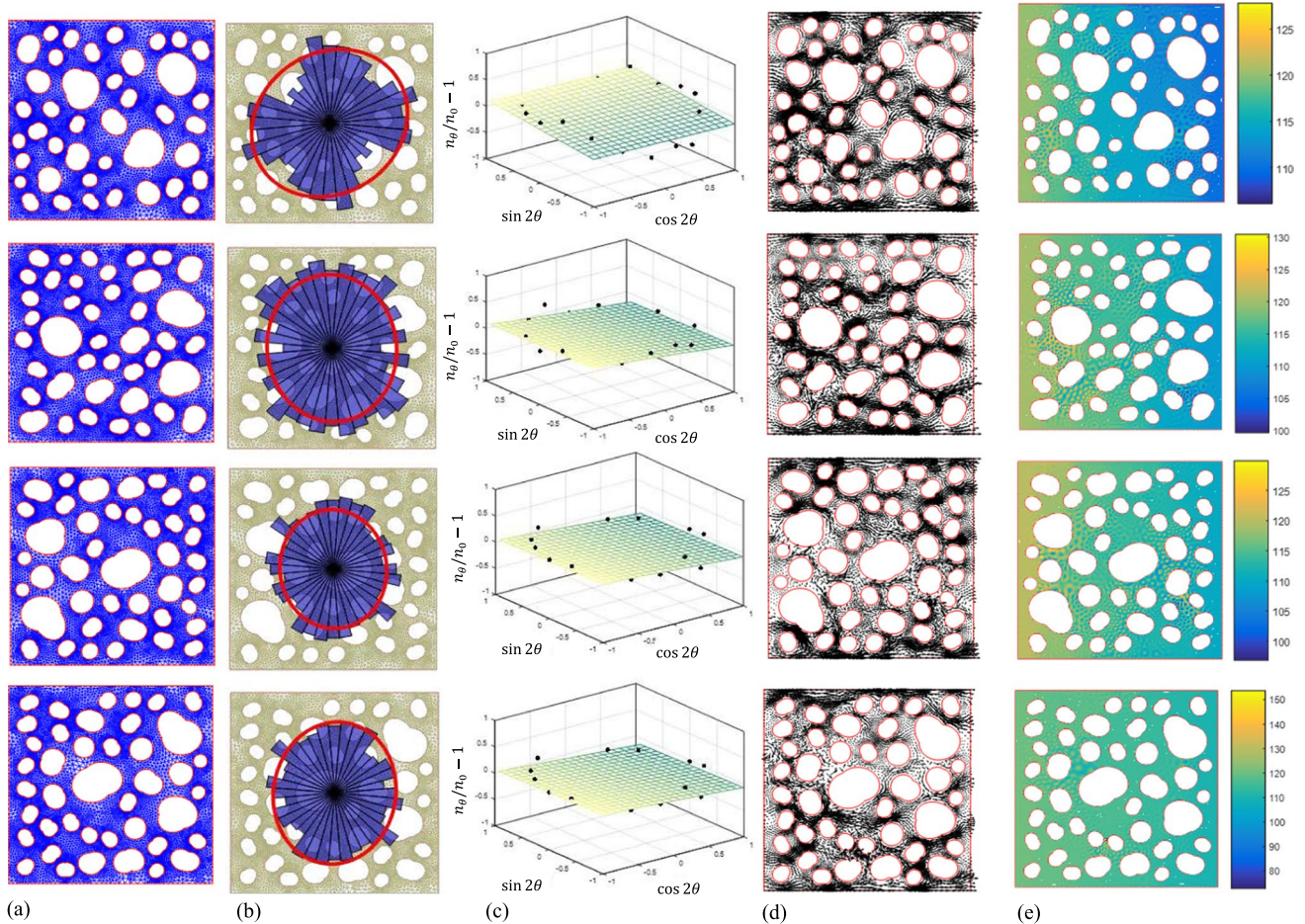


Fig. 6 Stokesian flow for various arrangements of particles and FE mesh for a constant porosity and GSD curve for Sample S2_a: **a** FE mesh for various arrangements of particles, **b** rose diagram **c** varia-

tions of the parameter $\eta = n^\theta/n_0 - 1$ with direction \mathbf{d} velocity field **e** pressure field (data from [25])

Once the Stokesian flow equation had been solved for the one-dimensional fluid flow in an isotropic domain, the hydraulic conductivity was calculated as follows:

$$k = \frac{v_{ave}}{i} \tag{8}$$

where v_{ave} is the average of the boundary velocities. For each case, the minimum, the maximum and the median hydraulic conductivities are calculated. Table 2 typically

shows some results for simulation of the experiments by Kedir [25] on S2_a sample. The finite element simulation, rose diagram for the variation of the normalized directional porosity parameter, $\eta = n^\theta/n_0 - 1$, velocity field and pressure field for some realizations are illustrated in Fig. 6. As stated earlier, all cases were analyzed under a constant, unit hydraulic gradient.

Table 3 shows a summary of the results for all simulations. In this table, a comparison with other empirical

Table 3 Comparison of the predicted, measured and empirical values of the one-dimensional hydraulic conductivity, $k(m/s)$, for different sands

Sand type	Porosity, n	Measured	Predicted	(1)	(2)	(3)	(4)	(5)	(6)	(7)
S2 _a	0.3809	3.5×10^{-4}	3.9×10^{-4}	1.3×10^{-3}	4.1×10^{-4}	1.4×10^{-3}	7.6×10^{-4}	1.1×10^{-4}	1.2×10^{-3}	5.1×10^{-4}
S8	0.4222	2.2×10^{-4}	2.8×10^{-4}	4.1×10^{-4}	1.5×10^{-4}	4.9×10^{-4}	2.0×10^{-4}	3.0×10^{-5}	3.7×10^{-4}	1.8×10^{-4}
S11	0.4157	2.7×10^{-4}	2.9×10^{-4}	7.5×10^{-4}	2.7×10^{-4}	8.6×10^{-4}	3.4×10^{-4}	4.0×10^{-4}	6.9×10^{-4}	3.3×10^{-4}
S12	0.3884	3.1×10^{-4}	3.0×10^{-4}	9.8×10^{-4}	3.2×10^{-4}	1.1×10^{-3}	4.2×10^{-4}	7.0×10^{-5}	9.1×10^{-4}	4.0×10^{-4}
SMPM	0.2930	4.1×10^{-4}	4.1×10^{-4}	5.0×10^{-4}	4.6×10^{-4}	4.3×10^{-4}	NA	NA	NA	4.2×10^{-4}
S6	0.3500	1.9×10^{-4}	2.7×10^{-4}	2.1×10^{-4}	6.0×10^{-5}	1.5×10^{-4}	3.4×10^{-4}	1.8×10^{-4}	2.2×10^{-4}	1.0×10^{-4}
S10	0.4100	1.5×10^{-4}	1.2×10^{-4}	4.1×10^{-4}	1.5×10^{-4}	4.5×10^{-4}	8.0×10^{-4}	3.9×10^{-4}	4.3×10^{-4}	2.6×10^{-4}
S2 _b	0.3660	9.1×10^{-4}	1.3×10^{-3}	NA	NA	NA	NA	NA	NA	NA

*NA not available

(1) Hazen [19] (2) Slichter [52] (3) Kozeny-Carman [4] (4) USBR [55] (5) Alyamani [1] (6) Breyer [28] (7) Terzaghi [39]

equations for the hydraulic conductivity has been made including the equations of Hazen [19], Slichter [52], Kozeny-Carman [4], USBR [55], Alyamani [1], Breyer [28] and Terzaghi [39]. According to this table, in most cases the hydraulic conductivity, calculated in this study, is close to the one proposed by Slichter [52] and in some cases it is close to that of Terzaghi [39] and USBR. Other equations exhibit less accuracy in prediction of the hydraulic conductivity.

Comparisons against measured data demonstrated a reasonable accuracy for the numerical simulations. The overall precision for all cases is fairly within $\pm 30\%$ which looks fine for the complicated problem of the fluid flow in porous media. In the following, anisotropic particle assemblies are produced to study their hydraulic conductivity. The degree of anisotropy in synthetic samples were controlled by looking at the rose diagram of the directional porosity at the end of each realization and a try-and-error procedure to achieve required degree of anisotropy.

It is important to note that the 1D *flow* does not mean a 1D *analysis*. In grain scale, a locally very complex 2D flow occurs in the REV which is macroscopically visualized as one-dimensional. Although no direct measurements on 2D flow has been made (at least not known to the authors) which may require elaborative experimental equipment, indirect verifications were made to show the capability of the proposed method, in particular, for 2D flow in anisotropic soils. Some, laboratory measurements along the maximum and minimum conductivities are available. This means that samples are tested along principal axes, i.e. the directional porosity, the microstructure and the hydraulic conductivity tensors are all diagonal, expressed in terms of their principal values.

The model was first calibrated along one direction only by changing the directional porosities in order to achieve an assemblage of particles with a consistent directional porosity (and the hydraulic conductivity) along the flow. The other value can be found by requiring the bulk porosity to be a fixed value and knowing that the 2D bulk porosity, $n_{2D} (\cong n^{2/3})$, is the determinant of the directional

Table 4 Two-dimensional analysis and verification for an anisotropic soil, SMPM (data from [46])

Flow direction (°)	Bulk porosity, n	Dry unit weight, γ_d (kN/m ³)	Measured values k_h and k_v (m/s)		Calibrated values k_h (m/s) and 2D principal directional porosities, n_h and n_v			Predicted values k_v (m/s)	
			k_h	k_v	k_h	n_h	n_v	k_h	k_v
0	0.2930	19.0	4.07×10^{-4}	2.26×10^{-4}	4.10×10^{-4}	0.7719	0.5730	–	2.1×10^{-4}
10	0.2930				–	–	–	4.00×10^{-4}	1.90×10^{-4}
20	0.2930				–	–	–	3.80×10^{-4}	2.00×10^{-4}
30	0.2930				–	–	–	3.60×10^{-4}	2.50×10^{-4}
0	0.3300	18.0	6.68×10^{-4}	3.55×10^{-4}	6.10×10^{-4}	0.8067	0.5902	–	3.70×10^{-4}
10	0.3300				–	–	–	6.90×10^{-4}	3.20×10^{-4}
20	0.3300				–	–	–	6.60×10^{-4}	3.50×10^{-4}
30	0.3300				–	–	–	6.10×10^{-4}	3.80×10^{-4}

*NA not available

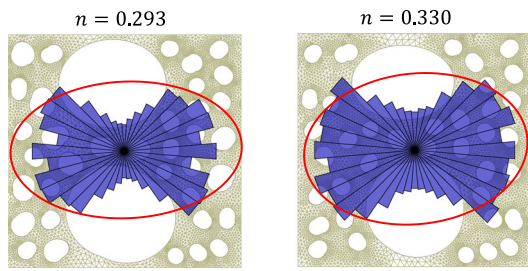


Fig. 7 Calibrated assemblage of particles for the experimental data of Qiu and Wang [46]

porosity tensor ($n_{2D} = \det \mathfrak{n} = n_h n_v$, where n_h and n_v are principal horizontal and vertical directional porosities). Therefore, a calibrated REV was found. In the next step, hydraulic gradients along different directions (say at 10° , 20° and 30° with respect to horizon) were introduced and the hydraulic conductivities were determined. Finally, the obtained hydraulic conductivity for the other principal direction and the mean value, (as a part of the hydraulic conductivity tensor), were then compared with the measured data.

Fortunately, for the sample SMPM, measurements are made for different porosities. We presented the results for two samples with $n = 0.293$ and $n = 0.330$ in Table 4 and Fig. 7. In this table, calibrated values correspond to one-dimensional (horizontal) flow. Once calibrations had been made, predicted values were obtained for arbitrary two-dimensional flow analyses. Results indicated that the numerical simulations are in reasonable agreement with experimental data.

8 Rational equation for the hydraulic conductivity of anisotropic soils

In this section, results of the numerical study on the hydraulic conductivity of anisotropic materials are presented. For this purpose, a number of realizations have been performed for each particular GSD curve with a fixed volumetric porosity but different degrees of anisotropy. The flow velocity under different hydraulic gradients of unit magnitude ($\|i\| = 1$) inclined at angles $\beta = 0, 10^\circ, 20^\circ, 30^\circ, 40^\circ$ and 90° are calculated.

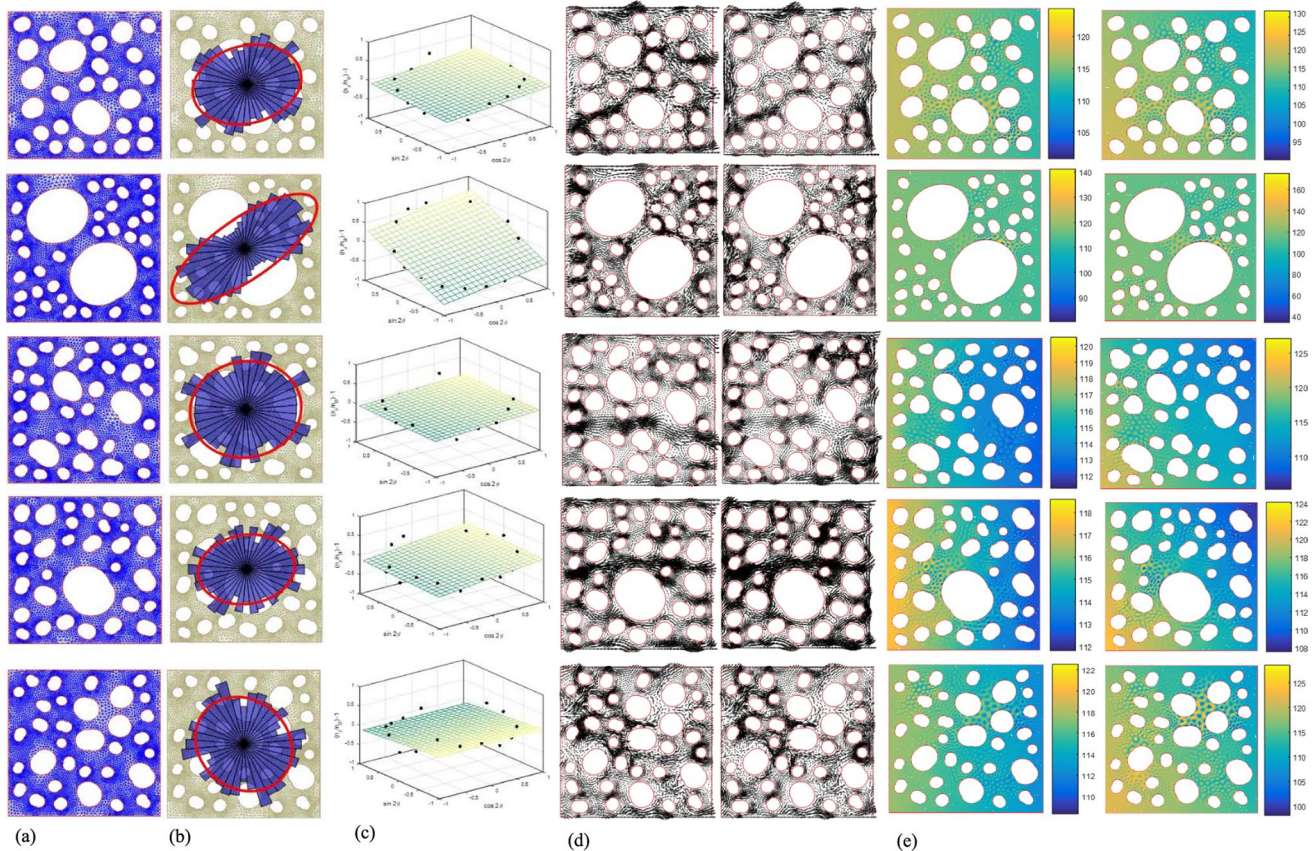


Fig. 8 **a** FE mesh for various arrangements of particles, **b** Rose diagram, **c** Variations of the parameter $\eta = n^\theta/n_0 - 1$ with direction **d** velocity field for $\beta = 0, \beta = 30^\circ$ **e** pressure field for $\beta = 0, \beta = 30^\circ$

Figure 8, demonstrates typical results for five different soil types, with a random assemblage of particles, under two different hydraulic gradients, i.e. with $\beta = 0$ and 30° . In this figure, the finite element mesh, the rose diagram and the distribution of the directional porosity, variations of the normalized parameter $\eta = n^\theta/n_0 - 1$ with direction, the velocity field and the pressure field, both corresponding to two different gradients, are presented. By conducting a number of analyses for a variety of microstructure tensors and hydraulic gradients for each soil type (with a fixed GSD curve and volumetric porosity), a database of the velocity vector versus the microstructure tensor is obtained which is a synthetic database for the rest of this work.

In the following, a rational relationship between the hydraulic conductivity and the microstructure tensor is investigated. It was stated that the hydraulic conductivity should be expressed as a 2nd order tensor, denoted by \mathbf{k} which is assumed to be a function of \mathfrak{F} . For the materials under study, i.e. clean medium to coarse sands with fairly round particles, such a dependence seems logical.

Some restrictions on the general form of this rational equation are originated from the representation theorem [49, 53] and the Cayley-Hamilton theorem [20]. Based on the representation theorem, the most general 3D form of a rational equation relating \mathbf{k} to \mathfrak{F} is as follows:

$$\mathbf{k} = \beta \mathbf{I} + \alpha \mathfrak{F}^M + \gamma \mathfrak{F}^{2M} \tag{9}$$

The general relationship is presented in terms of \mathfrak{F}^M where M is a positive integer. Constants α, β and γ are to be determined by the synthetic database. As required by the principle of objectivity and also the representation theorem, these constants must be functions of invariants of \mathfrak{F}^M . In addition, as required by the Cayley-Hamilton theorem, higher powers of \mathfrak{F}^M are unnecessary. It is worth noting that since no analytical solution is available, no exact relationship can be found between \mathbf{k} and \mathfrak{F} ; in other words, constants, as functions of invariants of \mathfrak{F}^M , can be taken arbitrarily. In addition, this equation should account for the isotropic condition if \mathfrak{F} reduces to a factor of \mathbf{I} . Therefore, the first term can be dropped. Now, partly for the sake of convenience and partly by inspection of different equations, by taking $M = 2$, the following simple linear relationship between \mathbf{k} and \mathfrak{F}^2 can be considered:

$$\mathbf{k} = \alpha \mathfrak{F}^2 \tag{10}$$

One may note that α is a function of invariants of \mathfrak{F}^2 (or equivalently, \mathfrak{r}^2) and not \mathfrak{F} (or \mathfrak{r}). Since the functional dependence of α and invariants of \mathfrak{F}^2 is quite general, it is very difficult to directly find such a relationship. Therefore, we first assumed a rational equation for α in terms of invariants of \mathfrak{F}^2 and tried to calibrate this equation to the observed numerical data. To do so, knowing that $\mathbf{v} = \alpha \mathfrak{F}^2 \mathbf{i}$, the results of a

series of analyses for a series of realizations under different hydraulic gradients of unit intensity ($\|\mathbf{i}\| = 1$) were inspected based on the database presented in previous section. In each case, the hydraulic gradient vector, \mathbf{i} , the microstructure tensor, \mathfrak{F} , and the velocity vector, \mathbf{v} , are known. Then, by introducing an equation for α in terms of invariants of \mathfrak{F}^2 (or \mathfrak{r}^2), this equation has been calibrated to attain a minimum error among all numerical simulations and predictions by the equation, $\mathbf{v} = \alpha \mathfrak{F}^2 \mathbf{i}$. This is done by assuming that for a particular assemblage of particles, a total number of m different unit hydraulic gradient vectors (at different angles) were introduced to the REV and velocities were numerically calculated.

Let us suppose that there are m simulations for m different unit hydraulic gradients in a particular anisotropic assemblage of particles. The velocities in each simulated REV can be found by the relation between \mathbf{k} and \mathfrak{F}^2 as follows, in two dimensions:

$$\begin{cases} v_1^{(1)} = \alpha_{\mathcal{J}11} i_1^{(1)} + \alpha_{\mathcal{J}12} i_2^{(1)} \\ v_2^{(1)} = \alpha_{\mathcal{J}21} i_1^{(1)} + \alpha_{\mathcal{J}22} i_2^{(1)} \end{cases}, \dots, \begin{cases} v_1^{(j)} = \alpha_{\mathcal{J}11} i_1^{(j)} + \alpha_{\mathcal{J}12} i_2^{(j)} \\ v_2^{(j)} = \alpha_{\mathcal{J}21} i_1^{(j)} + \alpha_{\mathcal{J}22} i_2^{(j)} \end{cases}, \dots, \begin{cases} v_1^{(m_s)} = \alpha_{\mathcal{J}11} i_1^{(m_s)} + \alpha_{\mathcal{J}12} i_2^{(m_s)} \\ v_2^{(m_s)} = \alpha_{\mathcal{J}21} i_1^{(m_s)} + \alpha_{\mathcal{J}22} i_2^{(m_s)} \end{cases}, \quad \text{where } \mathcal{J}_{ij} \triangleq \mathfrak{F}_{im} \mathfrak{F}_{mj} \tag{11}$$

In this equation, $v_1^{(j)}$ and $v_2^{(j)}$ are components of the velocity vector and $i_1^{(j)}$ and $i_2^{(j)}$ are components of the unit hydraulic gradient vector, in the j th simulation for a particular anisotropic assemblage of particles ($j = 1, 2, \dots, m_s$). In each assemblage, a total number of $2m_s$ equations for only one unknown, α , can be constituted. For this system of equation, the total error among all observations and predictions by the equation, for a particular anisotropic REV can be defined as:

$$E^{(s)} = \sum_{r=1}^m \frac{\left(v_1^{(r)} - \tilde{v}_1^{(r)}\right)^2 + \left(v_2^{(r)} - \tilde{v}_2^{(r)}\right)^2}{\|\tilde{\mathbf{v}}^{(r)}\|^2} \tag{12}$$

where $v_i^{(r)}$'s are calculated velocities by the FE simulations, $\tilde{v}_i^{(r)}$'s are those obtained by the hypothetical equation for α , s is an indicator for that particular assemblage and $i = 1, 2$.

The total error can be calculated for all anisotropic soil matrices under different hydraulic gradients, i.e. for all simulations, to attain the global minimum error. One should note that a particular form for α has been assumed a priori. Thus, a variety of different equations for α can be examined to attain the best agreement and the minimum error. In addition to the arbitrary form of such equations and their expression in rational form (i.e. in terms of invariants of \mathfrak{F}^2

or equivalently, α^2) this hypothetical form must satisfy the following restrictions and conditions. These conditions are partly physical and partly rational (or mathematical):

1. This equation should be expressed in terms of some power of n_0 , mathematically, it must be a homogeneous function of n_0 . This allows the representation of α to be converted from \mathfrak{F}^2 to α^2 and vice versa, by a constant factor.
2. The relationship should be exactly reducible to the isotropic condition, i.e. by tending \mathfrak{F} to $I/2$ this equation must be asymptotically approach to the one for isotropic materials. Although this restriction is perhaps not mandatory, it provides a quite general equation.
3. The equation must be physically meaningful and interpretable; for instance, increase in the mean porosity must increase the hydraulic conductivity.

By imposing these conditions and constraints and seeking for a simple and applicable form, after examining a variety of different equations, the final form of the equation for α has been found as follows, which meets all these conditions:

$$\alpha \cong \frac{1}{\sqrt{2}}f(I_1I_2, J_2), \frac{k}{k_0} = \alpha\mathfrak{F}^2, I_1, I_2, J_2 \tag{13a}$$

Invariants of \mathfrak{F}^2 (in 2 dimensions)

$$f(I_1I_2, J_2) = \sqrt{I_1} \left(\frac{\sqrt{|J_2|} + I_1}{I_2} \right), k_0 = \beta n_0(m/s) \tag{13b}$$

$$I_1 = \text{tr}\mathfrak{F}^2, I_2 = \det \mathfrak{F}^2, J_2 = \det \left(\mathfrak{F}^2 - \frac{1}{2}I_1\mathbf{I} \right) = I_2 - I_1^2/4 \tag{13c}$$

An estimate of the factor β is $4\sqrt{2} \times 10^{-4}(m/s)$ for the simulated data. It can be verified that by letting \mathfrak{F} approach $I/2$ (i.e. $J_2 \rightarrow 0$) the factor α tends to 4 (or $k/k_0 \rightarrow I$) which is required by this equation to be reducible to the one for isotropic materials. In addition, this equation is easily expressible in terms of α^2 . Note that J_2 is not independent in 2D flows, but this form was found to be simpler and more general.

Figure 9a shows variations of the factor α obtained numerically versus the function $f(I_1I_2, J_2)$ to achieve a linear relationship between α and $f(I_1I_2, J_2)$. In these simulations, about 75% of the measured data were used for model calibration (with a correlation factor of R^2 close to 0.84) while the rest were kept for verification. Results indicate that this equation complies reasonably with calculated data. One may note that the minimum value of $f(I_1I_2, J_2)$, corresponding to isotropic condition, is equal to 4. To further evaluate the ability of this rational equation in prediction of the hydraulic conductivity, components of the hydraulic conductivity tensors obtained by the finite element simulations in anisotropic assemblages of particles were compared with those predicted by the suggested equation. Results for different samples are plotted in Fig. 9b. All three components of k_{11}, k_{22} and $k_{12} = k_{21}$, normalized by k_0 , are plotted. Predictions made by the developed equation show a fairly good agreement with calculated data, considering difficulties in accurate measurement or calculation of the hydraulic conductivity in granular media.

This equation has been developed based on the database recompiled from anisotropic soils simulations. To increase

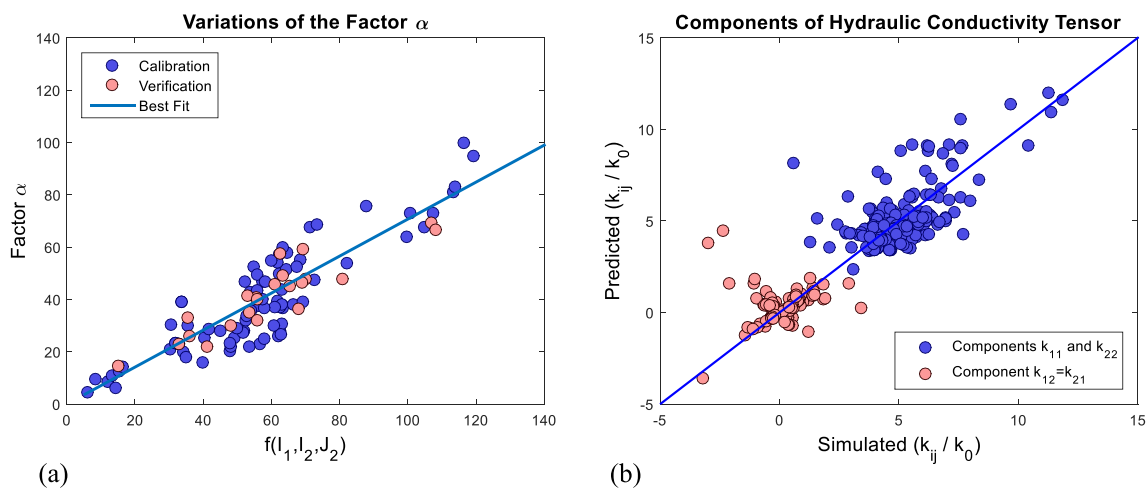


Fig. 9 **a** variations of the factor α with the function $f(I_1I_2, J_2) = \sqrt{I_1}(\frac{\sqrt{|J_2|} + I_1}{I_2})$ to achieve a linear relationship and **b** predicted and simulated hydraulic conductivities by the developed equation and numerical simulations

Table 5 Comparisons with some available experimental data for one-dimensional flow or isotropic samples

Sand type	Soil properties						k in one dimension		β_{exact} ($\times 10^4$)	References
	Volumetric porosity, n	D_{10}	D_{30}	D_{50}	D_{60}	C_u	Measured	Predicted**		
S2 _a	0.3809	0.34	0.62	0.98	1.18	3.5	3.5×10^{-4}	4.1×10^{-4}	$3.4\sqrt{2}$	Kedir [25]
S8	0.4222	0.17	0.23	0.29	0.34	2.0	2.2×10^{-4}	4.2×10^{-4}	$2.1\sqrt{2}$	Kedir [25]
S11	0.4157	0.24	0.34	0.47	0.53	2.2	2.7×10^{-4}	4.2×10^{-4}	$2.6\sqrt{2}$	Kedir [25]
S12	0.3884	0.29	0.49	0.76	0.92	3.2	3.1×10^{-4}	4.1×10^{-4}	$3.1\sqrt{2}$	Kedir [25]
SMPM	0.2930	0.15	1.00	2.50	4.20	28.0	4.1×10^{-4}	3.8×10^{-4}	$4.5\sqrt{2}$	Qiu and Wang [46]
S6	0.3500	0.14	0.20	0.29	0.34	2.4	1.9×10^{-4}	3.9×10^{-4}	$1.9\sqrt{2}$	Jaafar and Likos [23]
S10	0.4100	0.17	0.18	0.20	0.21	1.2	1.5×10^{-4}	4.2×10^{-4}	$1.4\sqrt{2}$	Nemes et al. [32]***
S2 _b	0.3660	0.30	0.51	0.99	1.04	3.5	9.1×10^{-4}	4.1×10^{-4}	$9.0\sqrt{2}$	Bouteldja et al. [2]
S1n	0.4400	0.26*	0.28	0.35	0.37	1.4	5.4×10^{-4}	4.3×10^{-4}	$5.0\sqrt{2}$	Nemes et al. [32]***
S2n	0.3500	0.14*	0.12	0.29	0.34	2.5	1.9×10^{-4}	3.8×10^{-4}	$1.9\sqrt{2}$	Nemes et al. [32]***
S3n	0.3000	0.15*	0.17	0.22	0.23	1.5	1.1×10^{-4}	3.7×10^{-4}	$1.2\sqrt{2}$	Nemes et al. [32]***
S4n	0.4100	0.11*	0.11	0.16	0.18	1.7	4.0×10^{-4}	4.2×10^{-4}	$3.8\sqrt{2}$	Nemes et al. [32]***
S5n	0.4100	0.11*	0.16	0.22	0.23	2.1	3.9×10^{-4}	4.2×10^{-4}	$3.7\sqrt{2}$	Olanrewaju and Wong (1994)

*For these samples D_{20} was reported instead of D_{30}

**By taking $k_0 \cong \beta n_0$

***Data recompiled by Jaafar and Lokos [23]

Table 6 Estimates of different measures of errors in approximating all components of the permeability tensor among simulations and suggested equation

Measure of error	Mean relative error	SD	RMSE
Value	0.34	0.13	0.31

the accuracy of the constant β , accounting for isotropic condition, a series of measured data on one-dimensional fluid flow in some sands are presented in Table 5 (including previous data plus some few more, i.e. S1n through S5n). This factor can be slightly modified to allow this equation to cover the range of data for the isotropic condition. Exact values of β fitted to experimental data, denoted by β_{exact} , is also presented. According to the range of β_{exact} , we would suggest $\beta \cong (2.0 \sim 5.0)\sqrt{2} \times 10^{-4} (m/s)$ to achieve better estimates. Unfortunately, the isotropy of the set of data reported in this table are not clarified and cannot be guaranteed; they are just 1D measurements on laboratory samples. In addition, in some cases the hydraulic gradient under which the test has been conducted is not known. Therefore, one may use other equations for the isotropic condition instead of the one we presented here for numerically simulated samples. Finally, Table 6, shows some measures of estimated errors in the entire range of data. Considering difficulties

in an appropriate estimate of the coefficient of permeability and discrepancies in experimental data or simulations, error measures seem to be reasonable for practical purposes. Higher accuracy may be obtained by including other factors at the cost of more complex analyses.

9 A note on significance and use

The proposed rational equation has been obtained based on a series of numerical simulations on a number of clean, uniformly graded medium to coarse sands. While the existing empirical equations often suffer from difficulties in finding quantities such as the tortuosity, threshold pore size, diameter of effective flow channel, etc., this rather simple equation requires only prescription of the geometric measure of anisotropy, \mathfrak{F} (also \approx or Ω). There are some practical indirect ways to estimate the microstructure tensor, \mathfrak{F} , beside direct measurements (such as X-ray photography). For instance, by assuming the validity of the suggested equation and knowing the direction of the sedimentation plane, only one hydraulic conductivity test can be conducted to find this tensor as the coincidence of the principal directions of \mathbf{k} , \approx and \approx^2 in addition to the relationship between n and \approx , leave a system of two equations into two unknowns. For cases where there is no information about the sedimentation planes, a set of two tests along two arbitrary directions is required (together

with the relation $n_{2D} = \det \mathfrak{N}$ to find the components of \mathfrak{N} (also \mathfrak{N} or \mathfrak{Q}). To make it clear, we present a summary of calculations for the dataset of Qiu and Wang [46] in Appendix 2 of this paper. The microstructure tensor can also be independently found by other tests as this is just a geometric measure of anisotropy and not a sole character of the hydraulic conductivity. For example, by considering some anisotropic failure criterion (if the anisotropy in strength is assumed to be the same as that for the hydraulic conductivity), a series of shear strength tests may be used to find components of this tensor with adequate accuracy. Further details can be found in Inglis and Pietruszczak [22], Oboudi [34] and Oboudi et al. [35].

10 Conclusions

The hydraulic conductivity of anisotropic sands was studied to find a tensorial form of the hydraulic conductivity tensor, limited to 2D flows. Although there are a number of different empirical equations for the hydraulic conductivity, there is no such relationship available for anisotropic soils. In addition, we showed that the hydraulic conductivity cannot be considered as a scalar value changing from one direction to another; but this is a 2nd order tensor quantity. To overcome difficulties in experimental tests, this research has been conducted based on numerical simulations of assemblages of particles which also allows accurate measurements on the geometric measure of anisotropy.

The concept of the microstructure tensor based on the directional porosity, as a geometric measure of anisotropy, has been employed. Practically, the microstructure tensor can be measured by direct or indirect methods. This measure has been calculated in REV's and once the Navier–Stokes equations have been numerically solved for all REV's the hydraulic conductivity has been related to the microstructure tensor. Although the hydraulic conductivity can be related to other factors such as the particles shape, porosity, magnitude of the hydraulic gradient, temperature, etc. this simple relationship is proved to be reasonable at least for a wide range of clean, uniformly graded medium sands (classified as SP) with nearly round particles at a unit hydraulic gradient. For such materials, the geometric measure of anisotropy which implicitly involves the porosity in its most general form, proves to be adequate to characterize the hydraulic conductivity. The procedure involves the development of a synthetic database for a series of REV's and using this database to find the rational equation for the hydraulic conductivity. To produce the

synthetic database, extensive verifications were also made. The developed equation also meets some required physical and mathematical constraints such as the reducibility to the isotropic state and rationality. Verifications with a number of simulated cases show that this equation can reasonably predict the hydraulic conductivity of anisotropic samples of sand in two dimensions. One may note that the suggested equation can be applied to uniformly graded medium sands with round particles. It should be noted that either the measurement or the determination/estimation of the hydraulic conductivity serve as very challenging tasks in soil mechanics, particularly in anisotropic media. Thus, studies on the hydraulic conductivity of anisotropic soils remain an open field of research.

Appendix 1

Here, we show that the following equation violates principles of continuum mechanics by deriving the correct form for it:

$$\frac{1}{k_r} = \frac{\cos^2 \alpha}{k_x} + \frac{\sin^2 \alpha}{k_y}, v_r = -k_r \partial h / \partial r, v_x = -k_x \partial h / \partial x, v_y = -k_y \partial h / \partial y$$

Without loss of generality, we assume Cartesian tensors and hence, the Darcy's law will be as follows:

$$v = -k \nabla h = \begin{pmatrix} k_{xx} & k_{xy} \\ k_{yx} & k_{yy} \end{pmatrix} \begin{pmatrix} \partial h / \partial x \\ \partial h / \partial y \end{pmatrix} \text{ or } v_i = -k_{ij} h_{,j}, h_{,j} = \partial h / \partial x_j$$

Therefore, the velocity vector in any Cartesian coordinates system must follow the following transformation rule:

$$\begin{aligned} v'_m &= a_{im} v_i = a_{im} (-k_{ip} h_{,p}) = a_{im} (-k_{ij} \delta_{jp} h_{,p}) \\ &= a_{im} (-k_{ij} a_{jn} a_{pn} h_{,p}) = -(a_{im} a_{jn} k_{ij}) (a_{pn} h_{,p}) = -k'_{mn} h'_{,n} \end{aligned}$$

with a_{ij} being the Cartesian coordinate transform tensor. Thus, the components of the hydraulic conductivity tensor, in the new coordinates system will be:

$$k'_{mn} = a_{im} a_{jn} k_{ij}$$

Again, without loss of generality, we further assume that the x and y directions are principal material directions, i.e. they coincide with the maximum and minimum hydraulic conductivities. These are typical assumptions in most standard texts on soil mechanics. The coordinates

transformation under an orthogonal transformation (from $x - y$ to $r - s$ coordinates) and hence, components of the hydraulic conductivity will be:

$$A = (a_{ij}) = \begin{pmatrix} \cos \alpha & -\sin \alpha \\ \sin \alpha & \cos \alpha \end{pmatrix},$$

$$k' = A^T k A = \begin{pmatrix} \cos \alpha & \sin \alpha \\ -\sin \alpha & \cos \alpha \end{pmatrix} \begin{pmatrix} k_x & 0 \\ 0 & k_y \end{pmatrix} \begin{pmatrix} \cos \alpha & -\sin \alpha \\ \sin \alpha & \cos \alpha \end{pmatrix}$$

As a result:

$$k_{rr} = k_x \cos^2 \alpha + k_y \sin^2 \alpha,$$

$$k_{rs} = k_{sr} = -k_x \cos \alpha \sin \alpha + k_y \cos \alpha \sin \alpha,$$

$$k_{ss} = k_x \sin^2 \alpha + k_y \cos^2 \alpha$$

Therefore, the hydraulic conductivity tensor obtained this way, will not violate principles of continuum mechanics. In other words, the Darcy’s equation, expressed in tensorial form, will remain unchanged under any such transformation. This equation is indeed different from the conventional equation based on the partial derivative of h with respect to r only. In other words, v_r depends not only on k_{rr} but also on k_{rs} .

Appendix 2

A summary of calculations to estimate the hydraulic conductivity tensor for an anisotropic soil is presented in order to show how to use Eqs. (10) and (13). Let us inspect the case where only the bedding plane is known with no direct information on the microstructure tensor. The experimental data of Qiu and Wang [46] is examined. We start by using the following set of experimental data, i.e. employing n and k_h while keeping k_v for verification:

$$n \cong 0.33, k_1 = k_h \cong 6.7 \times 10^{-4} m/s, (k_2 = k_v \cong 3.6 \times 10^{-4} m/s)$$

If the coordinates system is taken along the material axes, both n and \mathfrak{F} will become diagonal in the material coordinates system. By denoting the principal values of \mathfrak{F} by \mathfrak{F}_1 and \mathfrak{F}_2 and those for n by n_1 and n_2 , one may write:

$$k = \alpha k_0 \mathfrak{F}^2 = \alpha k_0 \begin{pmatrix} \mathfrak{F}_1 & 0 \\ \text{sym.} & \mathfrak{F}_2 \end{pmatrix}^2, \mathfrak{F} = n / \text{tr} n,$$

$$n = \begin{pmatrix} n_1 & 0 \\ \text{sym.} & n_2 \end{pmatrix}, \det n = n_{2D} = n^2/3$$

The invariants I_1, I_2 and J_2 of \mathfrak{F}^2 are $\mathfrak{F}_1^2 + \mathfrak{F}_2^2, \mathfrak{F}_1^2 \mathfrak{F}_2^2$ and $-(\mathfrak{F}_1^2 - \mathfrak{F}_2^2)^2/4$, respectively. Referring to Eq. (13) after some manipulations and substitution of \mathfrak{F}_1 and \mathfrak{F}_2 with n_1 and n_2 in the equation for α , one will get:

$$\alpha \mathfrak{F}_1^2 = \frac{\sqrt{n_1^2 + n_2^2}}{2\sqrt{2}n_2^2(n_1 + n_2)} (3n_1^2 + n_2^2)$$

$$= \frac{k_1}{\beta(n_1 + n_2)/2}$$

$$= \frac{6.7 \times 10^{-4}}{4\sqrt{2} \times 10^{-4}(n_1 + n_2)/2}, n_1 n_2 = n^2/3 \cong 0.48$$

Solution for n_1 and n_2 gives $n_1 \cong 0.81$ and $n_2 \cong 0.58$. Thus, the hydraulic conductivity tensor will be obtained:

$$n = \begin{pmatrix} 0.81 & 0 \\ 0 & 0.59 \end{pmatrix},$$

$$\mathfrak{F} = \begin{pmatrix} 0.58 & 0 \\ 0 & 0.42 \end{pmatrix},$$

$$\alpha \cong 5.1, k_0 \cong 4.0 \times 10^{-4} m/s,$$

$$k \cong \begin{pmatrix} 6.8 & 0 \\ 0 & 3.5 \end{pmatrix} \times 10^{-4} m/s$$

with $k_2 = k_v = 3.5 \times 10^{-4} m/s$ only slightly different from the experimental data (i.e. $3.6 \times 10^{-4} m/s$).

Here, knowing the orientation of the bedding plane and the constraint $\det n = n_{2D}$, only one independent component of n (or \mathfrak{F}) was required to be found. If the bedding plane is not known, at least two tests will be required to calculate the microstructure and the hydraulic conductivity tensors as, after applying the condition $\det n = n_{2D}$, there will be two independent components for n (or \mathfrak{F}).

Supplementary Information The online version contains supplementary material available at <https://doi.org/10.1007/s10035-023-01352-9>.

Acknowledgements The authors would like to draw their appreciation to Prof. Mojtaba Mahzoon (Professor Emeritus in Applied Mechanics

and Mathematics, School of Mechanical Engineering, Shiraz University) for his scientific support in tensor analysis and solution of systems of nonlinear PDEs.

Funding The authors received no fund for this research. This paper is an original work entirely conducted by a research team including the authors of this paper (and no one else) at the School of Engineering, Shiraz University.

Declarations

Conflict of interest There is no conflict of interest in this work with any others.

References

- Alyamani, M.S., Sen, Z.: Determination of hydraulic conductivity from grain-size distribution curves. *Ground Water* **31**(4), 551–555 (1993)
- Bouteldja, F., Breul, P., Boissier, D.: Experimental validation of a method for in situ estimation of hydraulic conductivity of water treatment granular materials. *Geotech Geological Eng* **29**, 1009–1021 (2011). <https://doi.org/10.1007/s10706-011-9433-x>
- Carman, P.C.: The determination of the specific surface of powders. *J Soc Chem Ind* **57**, 225–234 (1938)
- Carman, P.C.: Flow of gases through porous media. Butterworths Scientific Publications, London (1956)
- Chapuis, R.P.: Predicting the saturated hydraulic conductivity of sand and gravel using effective diameter and void ratio. *Can. Geotech. J.* **41**(5), 787–795 (2004). <https://doi.org/10.1139/T04-022>
- Chin, D.A.: Estimation of dispersion coefficients in porous media. *J. Hydraul. Eng. ASCE* **112**(7), 591–609 (1986). [https://doi.org/10.1061/\(ASCE\)0733-9429\(1986\)112:7\(591\)](https://doi.org/10.1061/(ASCE)0733-9429(1986)112:7(591))
- Churchill, R.V., Brown, J.W., Verhey, R.F.: Complex variables and applications. McGraw-Hill, New York (1974)
- Craig, C.F.: Soil Mechanics, 4th edn. Taylor and Francis Group, London (1987)
- Cushman, J.H.: On measurement, scale and scaling. *Water Resour. Res.* **22**(2), 129–134 (1986). <https://doi.org/10.1029/WR022i002p00129>
- Darcy, H.: Les Fontaines Publiques de la Ville de Dijon. Dalmont, Paris (1856)
- Das, B.M.: Advanced Soil Mechanics, 3rd edn. Taylor and Francis Group, London (1983)
- Fattah, Q.N., Hoopes, J.A.: Dispersion in anisotropic, homogeneous, porous media. *J. Hydraul. Eng. ASCE* **111**(5), 810–827 (1985). [https://doi.org/10.1061/\(ASCE\)0733-9429\(1985\)111:5\(810\)](https://doi.org/10.1061/(ASCE)0733-9429(1985)111:5(810))
- Fujikura, Y.: Estimation of permeability for sand and gravel based on pore-size distribution model. *J. Mater. Civ. Eng. ASCE* (2019). [https://doi.org/10.1061/\(ASCE\)MT.1943-5533.0002945](https://doi.org/10.1061/(ASCE)MT.1943-5533.0002945)
- Gad-el-Hak, M.: The fluid mechanics of microdevices: the free-man scholar lecture. *J. Fluids Eng. ASME* **121**(1), 5–33 (1999). <https://doi.org/10.1115/1.2822013>
- Ghabezloo, S., Sulem, J., Saint-Marc, J.: Evaluation of a permeability-porosity relationship in a low-permeability creeping material using a single transient test. *Int. J. Rock Mech. Min. Sci.* **46**(4), 761–768 (2009). <https://doi.org/10.1016/j.ijrmms.2008.10.003>
- Gray, W.G., Miller, C.T.: A generalization of averaging theorems for porous medium analysis. *Adv. Water Resour.* **62**(B), 227–237 (2013). <https://doi.org/10.1016/j.advwatres.2013.06.006>
- Gurtin, M.E., Fried, E., Anand, L.: The Mechanics and Thermodynamics of Continua. Cambridge University Press, UK (2010)
- Hassanizadeh, M., Gray, W.G.: General conservation equations for multi-phase systems: 1. Averaging procedure. *Adv. Water Resour.* **2**, 131–144 (1979). [https://doi.org/10.1016/0309-1708\(79\)90025-3](https://doi.org/10.1016/0309-1708(79)90025-3)
- Hazen, A.: Some physical properties of sands and gravels, with special reference to their use in filtration. In: 24th Annual Rep. Publication No. 34, Massachusetts State Board of Health, 539–556 (1892)
- Hoffman, K., Kunze, R.: Linear Algebra, 2nd edn. Prentice-Hall, Englewood Cliffs (1971)
- Hu, H., Braun, P., Delage, P., Ghabezloo, S.: Evaluation of anisotropic poroelastic properties and permeability of the opalinus clay using a single transient experiment. *Acta Geotech.* **16**, 2131–2142 (2021). <https://doi.org/10.1007/s11440-021-01147-3>
- Inglis, D., Pietruszczak, S.: Characterization of anisotropy in porous media by means of linear intercept measurements. *Int. J. Solids Struct.* **40**(5), 1243–1264 (2003). [https://doi.org/10.1016/S0020-7683\(02\)00595-4](https://doi.org/10.1016/S0020-7683(02)00595-4)
- Jaafar, R., Likos, W.J.: Pore-scale model for estimating saturated and unsaturated hydraulic conductivity from grain size distribution. *J. Geotech. Geoenviron. Eng. ASCE* (2014). [https://doi.org/10.1061/\(ASCE\)GT.1943-5606.0001031](https://doi.org/10.1061/(ASCE)GT.1943-5606.0001031)
- Kanatani, K.: Distribution of directional data and fabric tensors. *Int. J. Eng. Sci.* **22**(2), 149–164 (1984)
- Kedir, S.A.: Evaluation of hydraulic conductivity methods using laboratory, field and empirical equations: a case study in Mojo River Stream Bed. M.Sc., Addis Ababa Science and Technology University, Ethiopia, Thesis, (Supervisor: Argaw Asha) (2018)
- Kenney, T.C., Lau, D., Ofoegbu, G.I.: Permeability of compacted granular materials. *Can. Geotech. J.* **21**(4), 726–729 (1984)
- Kozeny, J.: Ueber kapillare Leitung Des Wassers Im Boden. *Wien, Akad. Wiss.* **136**(2a), 271 (1927)
- Kresic, N.: Quantitative Solutions in Hydrogeology and Groundwater Modeling. CRC Press, Boca Raton (1998)
- Mishra, G.C., Siva Reddy, A.: Exit gradient in anisotropic porous medium. *J. Hydraul. Eng. ASCE* **109**(6), 897–904. [https://doi.org/10.1061/\(ASCE\)0733-9429\(1983\)109:6\(897\)](https://doi.org/10.1061/(ASCE)0733-9429(1983)109:6(897)) (1983)
- Molaei, H., Veiskarami, M., Pietruszczak, S.: Localization of deformation in anisotropic granular materials utilizing the microstructure tensor. *Int. J. Geomech. ASCE* **21**(7), 55 (2021). [https://doi.org/10.1061/\(ASCE\)GM.1943-5622.0002015](https://doi.org/10.1061/(ASCE)GM.1943-5622.0002015)
- Moulton, L.K.: Highway Subdrainage Design. Federal Highway Administration Office of Research and Development, Washington, DC (1980)
- Nemes, A., Schapp, M.G., Leij, F.J.: UNSODA Database Version 2.0. USDA Agricultural Research Service, Washington DC, USA (1999)
- Neuman, S.P.: Theoretical derivation of Darcy's law. *Acta Mech.* **25**(3–4), 153–170 (1977). <https://doi.org/10.1007/BF01376989>
- Oboudi, M.: Characterization of inherent and induced anisotropy in granular materials, Ph.D. Dissertation (Supervised by S. Pietruszczak and A. G. Razaqpur), McMaster University, Hamilton, ON, Canada (2014)
- Oboudi, M., Pietruszczak, S., Razaqpur, A.G.: Description of inherent and induced anisotropy in granular media with particles of high sphericity. *Int. J. Geomech. ASCE* **16**(4), 04016006 (2016). [https://doi.org/10.1061/\(ASCE\)GM.1943-5622.0000635](https://doi.org/10.1061/(ASCE)GM.1943-5622.0000635)
- Oda, M.: Initial fabrics and their relations to mechanical properties of granular material. *Soils Found.* **12**(1), 18–36 (1972)
- Oda, M.: The mechanism of fabric changes during compressional deformation of sand. *Soils Found.* **12**(2), 1–18 (1972)
- Oda, M.: Inherent and induced anisotropy in plasticity theory of granular soils. *Mech. Mater.* **16**(1), 35–45 (1993)

39. Odong, J.: Evaluation of empirical formulae for determination of hydraulic conductivity based on grain-size analysis. *J. Am. Sci.* **3**(3), 54–60 (2007)
40. Pietruszczak, S.: *Fundamentals of Plasticity in Geomechanics*. CRC Press, London (2010)
41. Pietruszczak, S., Krucinski, S.: Considerations on soil response to the rotation of principal stress directions. *Comput. Geotech.* **8**(2), 89–110 (1989)
42. Pietruszczak, S., Krucinski, S.: Description of anisotropic response of clays using a tensorial measure of structural disorder. *Mech. Mater.* **8**(2), 237–249 (1989)
43. Pietruszczak, S., Mróz, Z.: Formulation of anisotropic failure criteria incorporating a microstructure tensor. *Comput. Geotech.* **26**(2), 105–112 (2000). [https://doi.org/10.1016/S0266-352X\(99\)00034-8](https://doi.org/10.1016/S0266-352X(99)00034-8)
44. Pietruszczak, S., Mróz, Z.: On failure criteria for anisotropic cohesive-frictional materials. *Int. J. Numer. Anal. Meth. Geomech.* **25**(5), 509–524 (2001). <https://doi.org/10.1002/nag.141>
45. Pietruszczak, S., Oboudi, M.: Description of induced anisotropy in microstructure of granular soils. *Soils Found.* **57**(4), 514–526 (2017). <https://doi.org/10.1016/j.sandf.2017.06.003>
46. Qiu, Z.-F., Wang, J.-J.: Experimental study on the anisotropic hydraulic conductivity of a sandstone-mudstone particle mixture. *J. Hydrol. Eng. ASCE* (2015). [https://doi.org/10.1061/\(ASCE\)HE.1943-5584.0001220](https://doi.org/10.1061/(ASCE)HE.1943-5584.0001220)
47. Ranaivomanana, H., Razakamanantsoa, A., Amiri, O.: Permeability prediction of soils including degree of compaction and microstructure. *International Journal of Geomechanics, ASCE* (2016). [https://doi.org/10.1061/\(ASCE\)GM.1943-5622.0000792](https://doi.org/10.1061/(ASCE)GM.1943-5622.0000792)
48. Reddy, J.N.: *An Introduction to the Finite Element Method*, 2nd edn. McGraw Hill, New York, NY (1993)
49. Rivlin, R.S., Ericksen, J.I.: Stress-deformation for isotropic materials. *J. Rat. Mech. Anal.* **4**, 323–425 (1955). https://doi.org/10.1007/978-1-4612-2416-7_61
50. Rosas, J., Lopez, O., Missimer, T.M., Coulibaly, K.M., Dehwah, A.H.A., Sesler, K., Lujan, L.R., Mantilla, D.: Determination of hydraulic conductivity from grain-size distribution for different depositional environments. *Ground Water* **52**(3), 399–413 (2014). <https://doi.org/10.1111/gwat.12078>
51. Saffman, P.G.: A theory of dispersion in a porous medium. *J. Fluid Mech.* **6**(3), 321–349 (1959). <https://doi.org/10.1017/S0022112059000672>
52. Slichter, C.S.: *Theoretical Investigation of the Motion of Ground Waters*. US. Geological Survey 19th Annual Rep., Part II, 295–384 (1898)
53. Truesdell, C.A., Noll, W.: *The Nonlinear Field Theories of Mechanics*. (Edited by Flügge). Springer, Berlin, Germany (1965)
54. Veiskarami, M., Roshanali, L., Habibagahi, G.: Effect of particles shape on the hydraulic conductivity of Stokesian flow in granular materials. *Geotech. Geol. Eng.* (2022). <https://doi.org/10.1007/s10706-022-02175-w>
55. Vukovic, M., Soro, A.: *Determination of Hydraulic Conductivity of Porous Media from Grain-Size Composition*. Littleton, CO, US (1992)
56. Whitaker, S.: Flow in porous media I: a theoretical derivation of Darcy's law. *Transp. Porous Media* **1**(1), 3–25 (1986). <https://doi.org/10.1007/BF01036523>
57. Zienkiewicz, O.C., Taylor, R.L.: *The Finite Element Method*, 5th edn. Butterworth Heinemann, Oxford (2005)

Publisher's Note Springer Nature remains neutral with regard to jurisdictional claims in published maps and institutional affiliations.

Springer Nature or its licensor (e.g. a society or other partner) holds exclusive rights to this article under a publishing agreement with the author(s) or other rightsholder(s); author self-archiving of the accepted manuscript version of this article is solely governed by the terms of such publishing agreement and applicable law.